Human Molecular Genetics, 2020, Vol. 29, No. 17 2951–2961

doi: 10.1093/hmg/ddaa178
Advance Access Publication Date: 21 August 2020
General Article

GENERAL ARTICLE

Prkar1a haploinsufficiency ameliorates the growth hormone excess phenotype in *Aip*-deficient mice

Marie Helene Schernthaner-Reiter[1,2,*,†], Giampaolo Trivellin[1,3], Thomas Roetzer[4], Johannes A. Hainfellner[4], Matthew F. Starost[5] and Constantine A. Stratakis[1]

[1]Section on Endocrinology and Genetics, *Eunice Kennedy Shriver* National Institute of Child Health and Human Development (NICHD), National Institutes of Health (NIH), Bethesda, MD 20892, USA, [2]Clinical Division of Endocrinology and Metabolism, Department of Internal Medicine III, Medical University of Vienna, 1090 Vienna, Austria, [3]Laboratory of Cellular and Molecular Endocrinology and Laboratory of Pharmacology and Brain Pathology, Humanitas Clinical and Research Center – IRCCS, 20089 Rozzano, Italy, [4]Division of Neuropathology and Neurochemistry, Department of Neurology, Medical University of Vienna, 1090 Vienna, Austria and [5]Office of Research Services (ORS), Division of Veterinary Resources (DVR), Office of the Director, National Institutes of Health, Bethesda, MD 20892, USA

*To whom correspondence should be addressed at: Clinical Division of Endocrinology and Metabolism, Department of Internal Medicine III, Medical University of Vienna, Waehringer Guertel 18-20, 1090 Vienna, Austria. Tel: 0043-1-40400-43110; Fax: 0043-1-40400-43090; Email: marie.schernthaner-reiter@meduniwien.ac.at

Abstract

Mutations of the regulatory subunit (*PRKAR1A*) of the cyclic adenosine monophosphate (cAMP)-dependent protein kinase (PKA), leading to activation of the PKA pathway, are the genetic cause of Carney complex which is frequently accompanied by somatotroph tumors. Aryl hydrocarbon receptor-interacting protein (*AIP*) mutations lead to somatotroph tumorigenesis in mice and humans. The mechanisms of *AIP*-dependent pituitary tumorigenesis are still under investigation and evidence points to a connection between the AIP and PKA pathways. In this study, we explore the combined effects of *Aip* and *Prkar1a* deficiency on mouse phenotype and, specifically, pituitary histopathology. $Aip^{+/-}$ mice were compared with double heterozygous $Aip^{+/-}$, $Prkar1a^{+/-}$ mice. The phenotype (including histopathology and serological studies) was recorded at 3, 6, 9 and 12 months of age. Detailed pituitary histological and immunohistochemical studies were performed at 12 months. Twelve-month old $Aip^{+/-}$ mice demonstrated phenotypic and biochemical evidence of GH excess including significantly elevated insulin-like growth factor 1 levels, larger weight and body length, higher hemoglobin and cholesterol levels and a higher frequency of growth plate thickening in comparison to $Aip^{+/}$, $Prkar1a^{+/-}$ mice. Pituitary histopathology did not uncover any pituitary adenomas or somatotroph hyperplasia in either group. These results demonstrate a slow progression from elevated GH release to the formation of overt somatotropinomas in $Aip^{+/-}$ mice; the acromegalic phenotype of these mice is surprisingly ameliorated in $Aip^{+/-}$, $Prkar1a^{+/-}$ mice. This highlights the complexities of interaction between the AIP and PKA pathway. Specifically targeting GH secretion rather than somatotroph proliferation may be an advantage in the medical treatment of *AIP*-dependent human acromegaly.

[†]Marie Helene Schernthaner-Reiter, http://orcid.org/0000-0002-7972-7610
Received: May 30, 2020. **Revised:** July 10, 2020. **Accepted:** July 15, 2020

Introduction

Pituitary adenomas are known to possess specific characteristics that distinguish them from other tumors: While they can cause deleterious effects, significant comorbidities and increased mortality due to stimulation or suppression of pituitary hormone secretion, and may exert local space occupying effects, they are rarely malignant (1). Thus, the natural history of pituitary tumors could be governed by unique molecular pathways that could be elucidated by the study of hereditary predisposition to pituitary tumors. A subset of familial isolated pituitary adenomas (FIPAs, OMIM #102200) is caused by inactivating mutations in the aryl hydrocarbon receptor-interacting protein (*AIP*) (2,3). Aip heterozygosity ($Aip^{+/-}$) in mice leads to a phenotype similar to the one observed in human *AIP* mutated ($AIPmut^{+}$) FIPA patients (4). $Aip^{+/-}$ mice were shown to develop pituitary adenomas, mostly somatotropinomas, that reach full penetrance by the age of 15 months (4).

The cyclic adenosine monophosphate (cAMP)-dependent protein kinase (PKA) pathway has been shown to be deregulated in sporadic pituitary adenomas, which commonly display activating somatic mutations of the $G_s\alpha$ subunit (encoded by the *GNAS* gene) (5,6). In addition, some genetic conditions that manifest with pituitary tumors also demonstrate alterations in the PKA pathway. Carney complex (OMIM #160980), which can lead to somatotropinomas or prolactinomas, is due to germline inactivating mutations in the R1α regulatory subunit of the PKA (encoded by the *PRKAR1A* gene) (7,8). $Prkar1a^{+/-}$ mice have a phenotype resembling human Carney complex patients to some extent, demonstrating bone tumors, Schwannomas and thyroid neoplasms, but they do not develop pituitary tumors (9). Pituitary-specific *Prkar1a* knockout mice, however, do exhibit an increased incidence of growth hormone (GH)-secreting pituitary adenomas (10). $Prkar1a^{+/-}$ mice bred within a background of hemizygosity for the known tumor suppressor gene *Rb1* also develop pituitary adenomas (11), demonstrating that *Prkar1a* haploinsufficiency may be a weak but definitely tumorigenic signal in the pituitary, especially when combined with other genetic defects.

While the detailed mechanisms of *AIP*-dependent pituitary tumorigenesis are currently still being investigated, AIP is known to physically and functionally interact with components of the PKA pathway including phosphodiesterases, G proteins and the catalytic and regulatory subunits of the PKA (12–18). Since both *Aip* heterozygosity and *Prkar1a* haploinsufficiency in mice contribute to pituitary tumorigenesis, we sought to investigate the combined phenotypic effects of *Aip* and *Prkar1a* heterozygosity in mice.

Results

Double heterozygous $Aip^{+/-}$, $Prkar1a^{+/-}$ mice are lighter and shorter than single heterozygous Aip mice

Body weight, body and tail length and organ weights were recorded. Male double heterozygous $Aip^{+/-}$, $Prkar1a^{+/-}$ (Aip/R1α) mice were significantly lighter than their single heterozygous $Aip^{+/-}$ (Aip) littermates at 10 and 11 months of age (Fig. 1A). Female Aip mice were also heavier than Aip/R1α mice at 10–12 months of age, but this difference did not reach statistical significance (Fig. 1B). Similarly, body lengths and tail lengths of Aip/R1α mice were shorter than those of single heterozygous Aip mice (Fig. 1C for male mice and Fig. 1D and E for females).

Male Aip mice at age 12 months had significantly higher thymus weights compared with male Aip/R1α mice (Supplementary Material, Fig. S2); no differences in thymus weights of males at other ages or in female mice were detected (data not shown). There was a trend toward higher liver weights in 12-month-old Aip mice of both sexes; however, this did not reach statistical significance ($P = 0.120$ for males and 0.371 for females, Supplementary Material, Fig. S2).

Double heterozygous $Aip^{+/-}$, $Prkar1a^{+/-}$ mice have reduced biochemical markers of growth hormone excess

Hematology showed significantly higher red blood cell (RBC) counts (Fig. 2A) and hemoglobin (HB) levels (Fig. 2B) in 12-month-old single heterozygous Aip compared with their double heterozygous Aip/R1α littermates. No significant differences in these parameters were detected at other ages (data not shown). Clinical chemistry analyses demonstrated significantly higher serum cholesterol in 12-month-old Aip mice (Fig. 2C) and significantly elevated triglycerides at the ages of 3, 9 and 12 months in Aip mice (Fig. 2D); serum glucose was also higher, but this difference did not reach statistical significance (Fig. 2E, $P = 0.10$). Conversely, serum alkaline phosphatase was higher in Aip/R1α mice compared with Aip mice (Fig. 2F); no significant differences were detected in the levels of hepatic transaminases, cholestasis parameters or parameters of hepatic synthetic function (data not shown). In terms of serum insulin-like growth factor 1 (IGF-1), a trend toward higher IGF-1 levels in Aip mice was already visible at the age of 28 weeks ($P = 0.054$), reaching statistical significance at age 49 weeks ($P = 0.001$, Fig. 2G). When male and female mice were analyzed separately, there were significantly higher levels of serum IGF-1 at 49 weeks in both male and female Aip mice, with a seemingly more pronounced difference in the males (158% in males versus 120% in females compared with IGF-1 levels measured in Aip/R1α mice; Supplementary Material, Fig. S2C and D). A two-way analysis of variance (ANOVA) showed significant between-subjects effects in terms of genotype ($P < 0.001$) but not in terms of gender ($P = 0.235$).

Aip mice have a higher frequency of thickened growth plates

Histopathological analysis of Aip mice in comparison to Aip/R1α mice revealed a significantly higher frequency of thickened growth plates in tibial bones of male and female Aip mice at 12 months of age ($P = 0.049$, Fig. 3A). Growth plate thickening, although it did not reach statistical significance, was also noted in femoral and humeral bones as well as vertebrate bodies of 12-month-old Aip mice (Fig. 3A and B). Growth plate thickening was not observed in any 3-month-old mice, whereas 6- and 9-month-old mice did not exhibit significant differences in the frequency of thickened growth plates (Supplementary Material, Fig. S2E and F, respectively).

Histopathology also demonstrated basophilic hypertrophic foci in the parotid and mandibular salivary glands of both Aip and Aip/R1α mice at all ages. In addition, phenotypic changes that had previously been noted in $Prkar1a^{+/-}$ mice were also observed in our Aip/R1α mice, including hepatic eosinophilic foci, splenic sinusoidal ectasia and numerous bone abnormalities, in particular osteofibrous dysplasias ($n = 9$, 81.8%) and osteofibromyxomas ($n = 6$, 54.5%) of the tail.

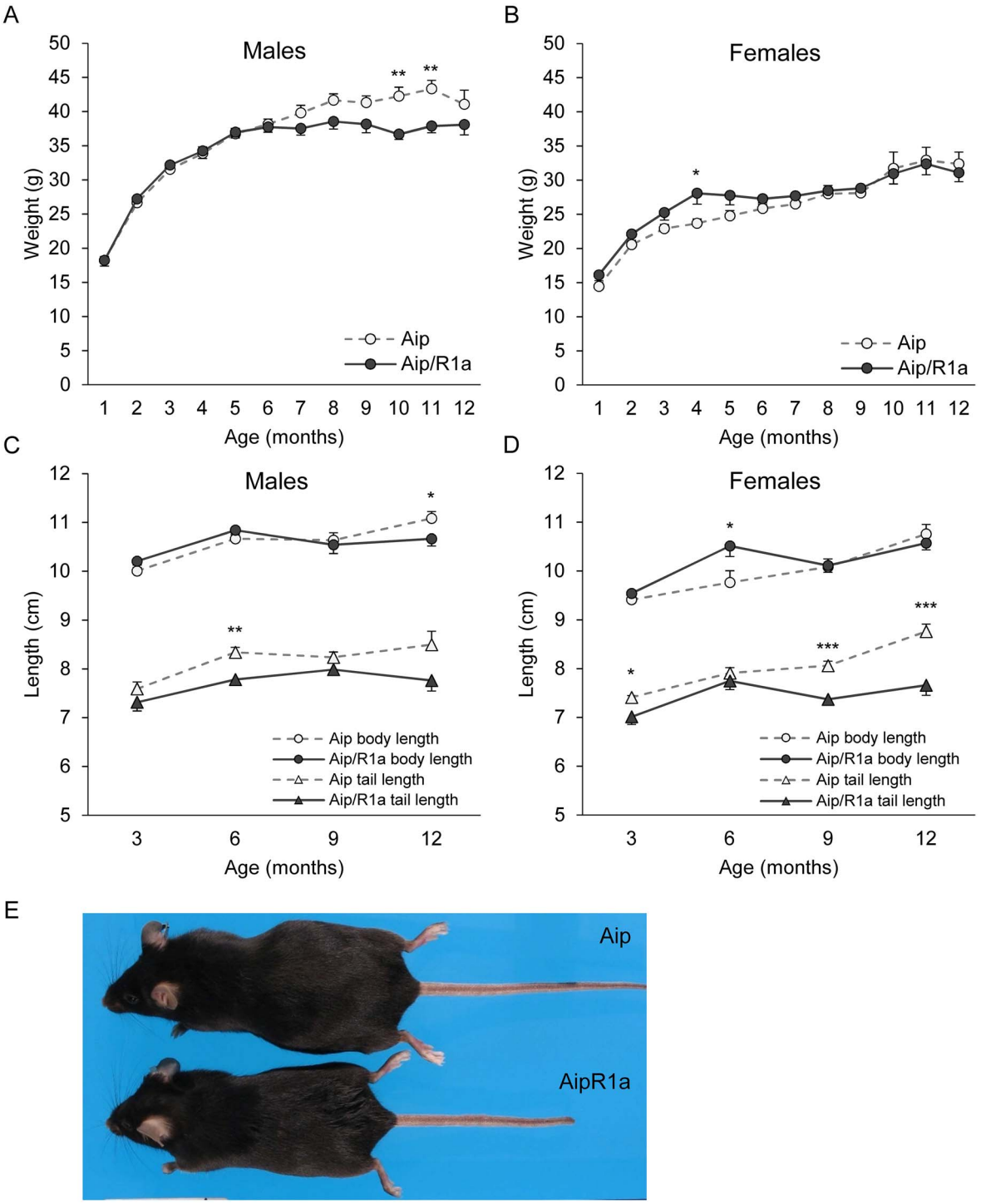

Figure 1. Weight, body and tail length of $Aip^{+/-}$ (Aip) and $Aip^{+/-}$, $Prkar1a^{+/-}$ (Aip/R1α) mice. Monthly weights of (**A**) male and (**B**) female Aip and Aip/R1α mice. Body and tail lengths of (**C**) male and (**D**) female Aip and Aip/R1α mice. (**E**) An example of two female 12-month-old littermates, with the single heterozygote (Aip) at the top and the double heterozygote (Aip/R1α) at the bottom. Data shown are means ± standard error of the mean, differences between means were tested with independent samples Student's *t*-tests or Mann–Whitney tests as appropriate. $^{*}P < 0.05$, $^{**}P < 0.01$, $^{***}P < 0.001$.

Pituitary histology and immunohistochemistry

Pituitary histopathology and immunohistochemistry were studied in Aip ($n = 12$) and Aip/R1α ($n = 11$) mice at 12 months of age. We did not observe overt pituitary tumors or consistent signs of hyperplasia; some female Aip mice ($n = 3$) showed scattered mitoses (Supplementary Material, Fig. S3A and B).

Pituitary GH staining was performed in most 12-month-old Aip ($n = 9$) and Aip/R1α ($n = 9$) animals. To quantify expression,

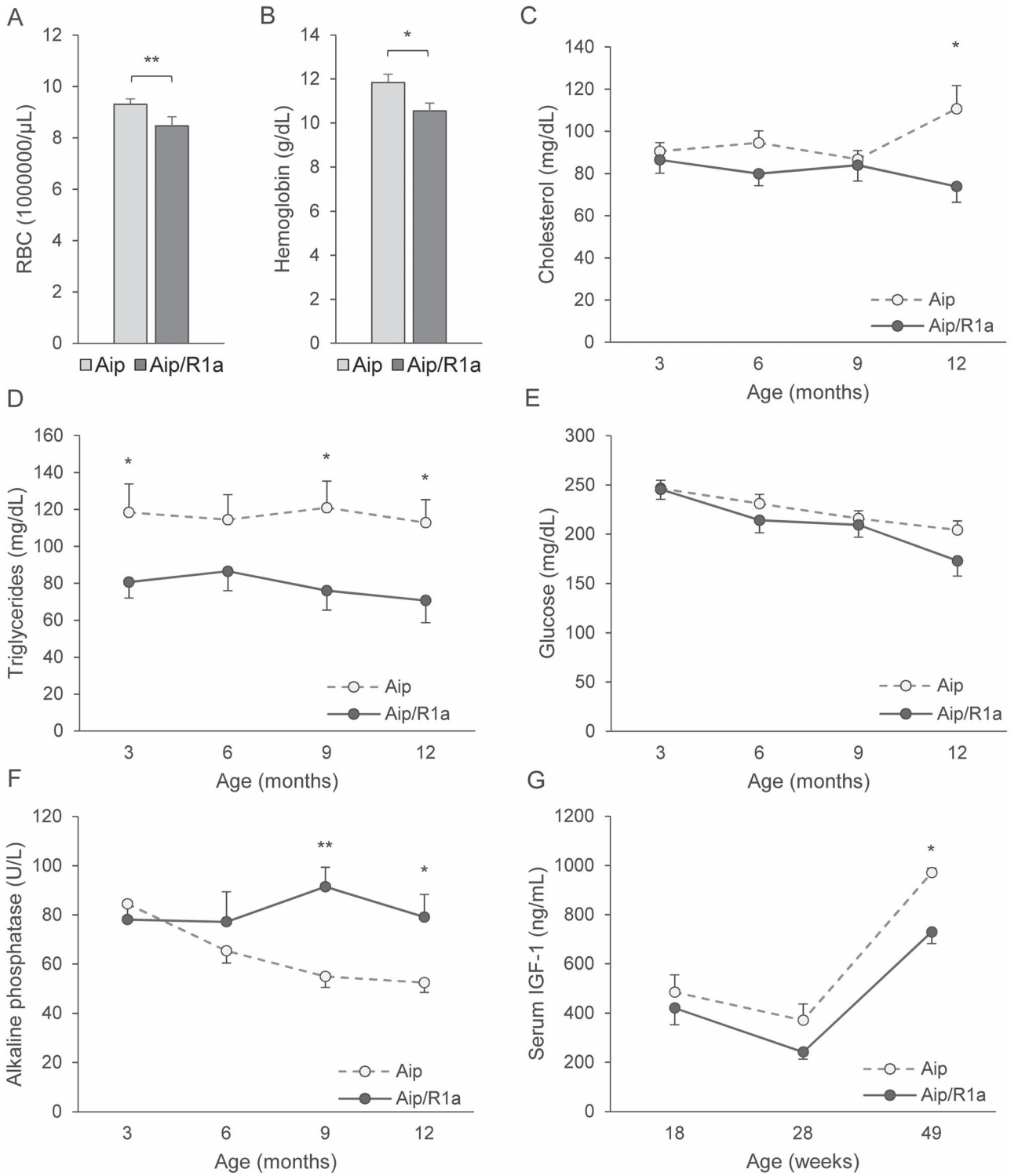

Figure 2. Hematology, clinical chemistry and serum insulin-like growth factor 1 (IGF-1) levels in $Aip^{+/-}$ (Aip) and $Aip^{+/-}$, $Prkar1a^{+/-}$ (Aip/R1α) mice of different ages. Red blood cell count (RBC, **A**) and hemoglobin levels (**B**) in 12-month-old mice. Serum cholesterol (**C**), triglycerides (**D**), glucose (**E**), alkaline phosphatase (**F**) and IGF-1 levels (**G**) in mice at different time points. Data shown are means ± standard error of the mean, differences between means were tested with independent samples Student's *t*-tests or Mann–Whitney tests as appropriate. $^{*}P < 0.05$, $^{**}P < 0.01$.

staining intensity was rated by two independent blinded viewers. Neither qualitative (Fig. 4A–F) nor semi-quantitative (Fig. 4G) differences in GH expression patterns were detected in Aip animals compared with Aip/R1α animals. Eosinophilia and cell proliferation by Ki67 positivity were also rated on semi-quantitative scales, which revealed no significant differences between Aip and Aip/R1α mice (Supplementary Material, Fig. S3C).

To estimate the PKA pathway activity, phosphorylated cAMP responsive element binding protein [phospho-CREB (cAMP responsive element binding protein)] immunofluorescence

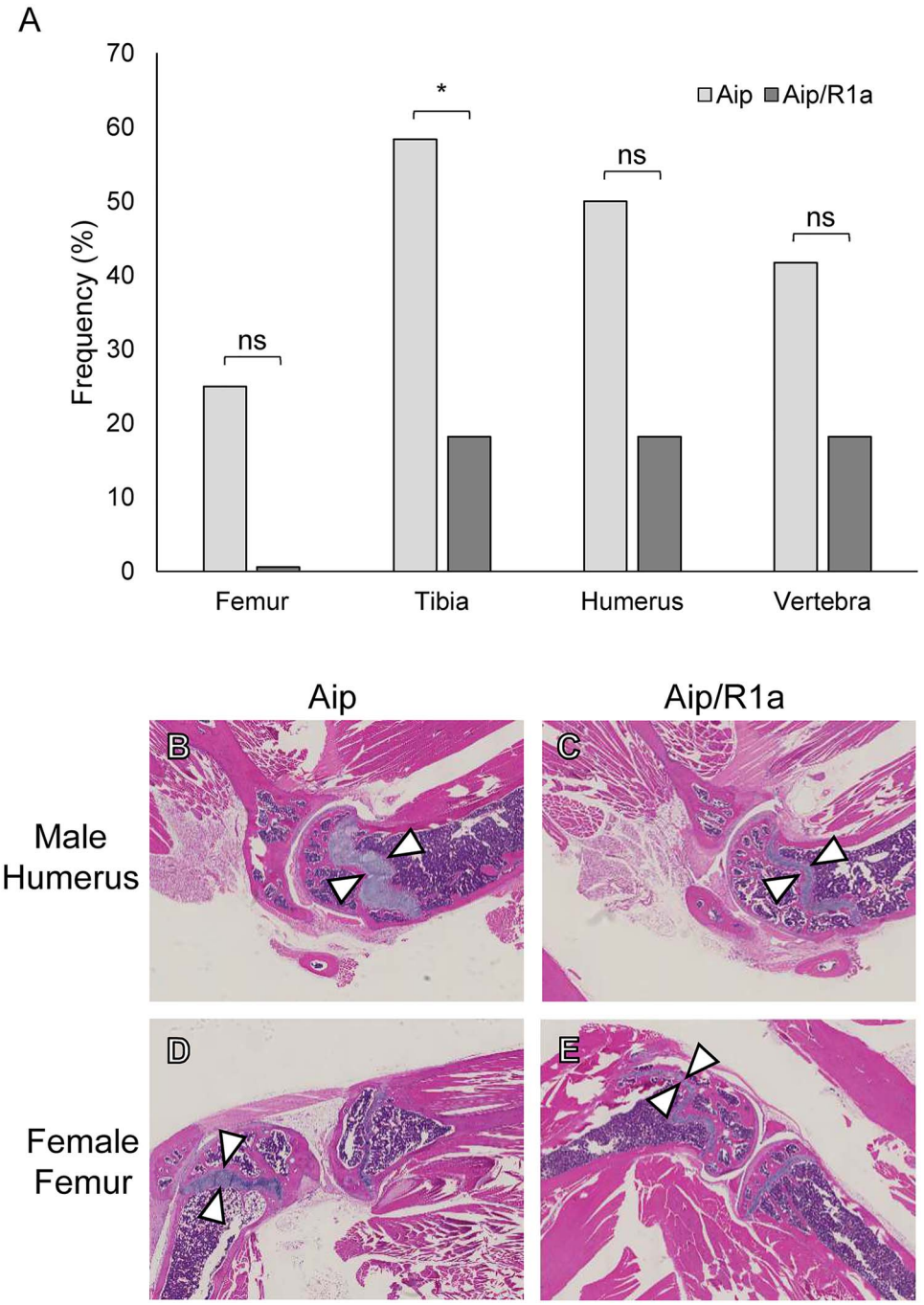

Figure 3. Growth plate thickness in $Aip^{+/-}$ (Aip) and $Aip^{+/-}$, $Prkar1a^{+/-}$ (Aip/R1α) mice. (**A**) Frequencies of thickened growth plates in 12-month-old male and female Aip ($n = 12$) and Aip/R1α ($n = 11$) mice in different bones. (**B–E**) H&E stained slides of Aip (B, D) and Aip/R1α (C, E) animals: humerus in two male animals (B, C) and femur in two female (D, E) animals. Growth plates are indicated with white arrowheads. Differences in frequencies between groups were tested with Pearson's Chi-squared tests. ns, not significant, $^*P < 0.05$.

(Supplementary Material, Fig. S3D–F and H–J) as well as cAMP staining (Supplementary Material, Fig. S3G and K) were performed on a subset of sections from 12-month-old Aip ($n = 3$) and Aip/R1α ($n = 3$); no difference in staining pattern or intensity was observed between those groups.

Discussion

We studied in detail the phenotype and pituitary histopathology of double heterozygous $Aip^{+/-}$, $Prkar1a^{+/-}$ (Aip/R1α) mice in comparison to single heterozygous $Aip^{+/-}$ (Aip) mice. We unexpectedly found that Aip/R1α mice do not present biochemical and phenotypic evidence of GH excess like the Aip mice. Aip mice demonstrated larger weight and body length, higher RBC and HB levels, higher cholesterol, triglycerides and a trend toward higher glucose levels, higher circulating IGF-1 levels, higher thymus weight, and a higher frequency of growth plate thickening.

The phenotypic changes we observed in Aip compared with Aip/R1α mice are similar to the clinical characteristics of

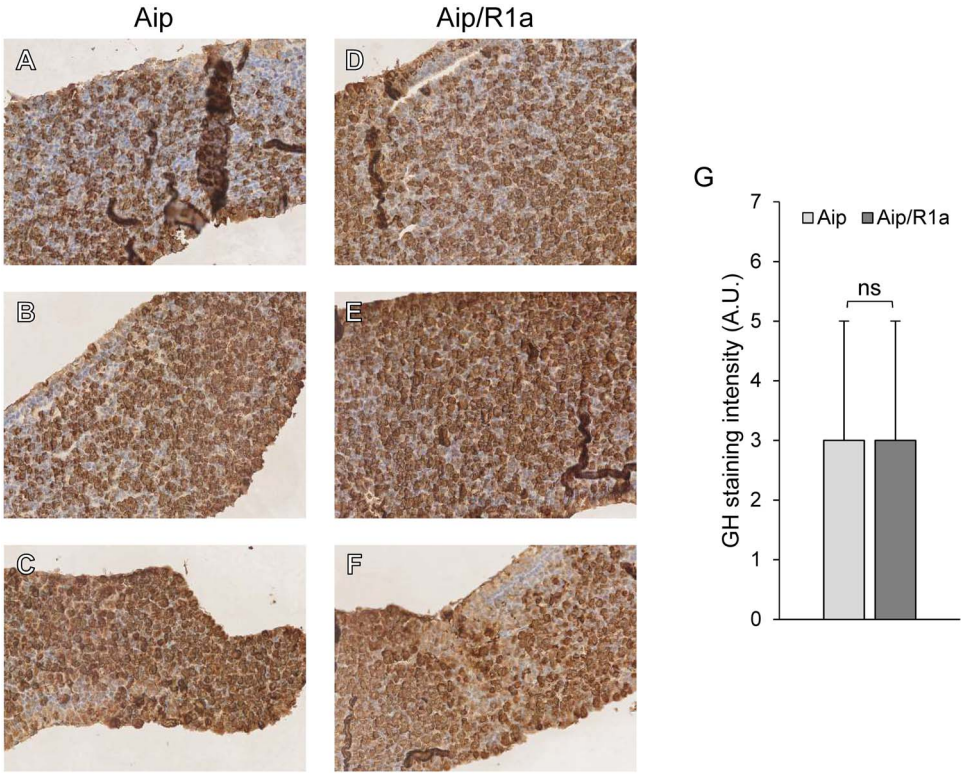

Figure 4. Pituitary histopathology. (**A–F**) Pituitary growth hormone (GH) immunohistochemistry in different 12-month-old in $Aip^{+/-}$ (Aip, A-C) and $Aip^{+/-}$, $R1a^{+/-}$ (Aip/R1α, D–F) mice. (**G**) Summary of results (medians ± interquartile range) from semi-quantitative staining intensity evaluation of GH expression in pituitaries of Aip ($n = 9$) and Aip/R1α ($n = 9$) mice. ns, not significant, A.U., arbitrary units.

human subjects with acromegaly and gigantism. Rapid growth and increased body length is typical of gigantism in humans and appears before the closure of the epiphyseal plate (19). In contrast to humans, mice do not undergo epiphyseal fusion at the time of sexual maturation (20) and continuously increased longitudinal growth and body weight is well documented in mouse models of acromegaly (21). In our male Aip mice, increased body weight became apparent at the age of 7 months and significant differences between groups were detected at 10 and 11 months (Fig. 1A), while body length was significantly increased at 12 months of age (Fig. 1C). Estrogen inhibits GH action and longitudinal growth, while testosterone enhances GH secretion and responsiveness (20,22), which may explain an amelioration of the growth phenotype in our female mice (i.e. the lack of significant difference in body length and body weight). In addition, we observed a lower apparent difference in IGF-1 levels between Aip and Aip/R1α mice in 49-week-old females (Supplementary Material, Fig. S2C and D), even though the interaction term between gender and genotype in two-way ANOVA did not reach statistical significance. An increased frequency of growth plate thickening even in our 12-month-old Aip mice (Fig. 3) also suggests increased stimulation of longitudinal growth in these mice (23). Thickened articular cartilages due to increased local and systemic IGF-1 production are a hallmark of human acromegaly, and they are related to disease activity (24). Our female Aip/R1α mice were significantly heavier than their Aip littermates at 4 months of age (Fig. 1B) and showed a longer body length at 6 months of age (Fig. 1D). This transient difference may be due to a different timing of growth spurts/plateaus in combination with a different body composition in acromegalic mice; GH transgenic mice were shown to be leaner than their wild-type (wt) littermates starting from ages 4–6 months but not at earlier ages (21).

Acromegaly is frequently accompanied by metabolic comorbidities including type 2 diabetes and dyslipidemia. Mouse models of acromegaly demonstrated normoglycemia but impaired glucose tolerance (25). While elevated serum cholesterol was found on a normal as well as a high-fat diet, serum triglycerides in GH transgenic acromegalic mice were normal under a normal diet and elevated on a high-fat diet (26,27). We detected a tendency toward elevated glucose and significantly elevated cholesterol as well as triglycerides in our 12-month-old Aip mice (Fig. 2), which was accompanied by a tendency toward higher liver weight in those animals (Supplementary Material, Fig. S2). Interestingly, cholesterol and triglyceride levels showed a different time course, with increased triglyceride levels at all ages (Fig. 2E), and increased cholesterol only at 12 months (Fig. 2D) in Aip mice. In human acromegaly, hypertriglyceridemia is frequently observed, whereas the rate of hypercholesterolemia is similar to that of the general population (28). In wt mice on a standard chow diet, normal values for triglycerides quoted between 85 and 120 mg/dL and for cholesterol at around 75–100 mg/dL (26,29,30); however, these are highly variable. In terms of cholesterol, however, these normal values correspond to the values observed in our Aip/R1α mice and suggest a pathologically elevated serum cholesterol in Aip mice. To our knowledge, this metabolic phenotype has not been described previously in $Aip^{+/-}$ mice (4,31,32) or $Aip^{-/-}$ mice (33).

We found increased thymus weights in our 12-month-old Aip mice (Supplementary Material, Fig. S1), whereas there were no differences between groups in white cell or lymphocyte counts (data not shown). Interestingly, a reversal of thymic aging (as well

as increased extramedullary hematopoiesis) was shown for aged rats with subcutaneously implanted GH3 cells which secrete GH (34,35), while a higher number of thymic Hassall's corpuscles was detected in advanced human acromegaly (36).

Our Aip mice demonstrated a significantly higher hemoglobin as well as red blood cell count compared with Aip/R1α mice. GH and IGF-1 have been shown to stimulate erythropoiesis *in vitro*, in mice and in humans with GH deficiency (37–39); acromegaly in humans is associated with increased red cell mass (40). On the other hand, erythropoiesis mainly occurs in the bone marrow, and this process may be impaired due to the bone tumors present in Aip/R1α mice. Similarly, we would attribute the higher alkaline phosphatase levels in Aip/R1α mice to the higher tumor load in this group (9).

Significantly, while our Aip mice at 12 months of age displayed an acromegalic phenotype and demonstrated elevated IGF-1 levels (Fig. 2G), we did not detect any pituitary histological abnormalities indicating somatotropinoma formation or somatotroph hyperplasia.

To ascertain this finding, we performed a number of additional stains and semi-quantitative measurements (GH staining and quantitation, cell proliferation by Ki67 staining, estimation of acidophil cell prevalence by quantitation of eosinophilia, estimation of PKA pathway activity by phospho-CREB immunofluorescence and cAMP staining, Fig. 4 and Supplementary Material, Fig. S3) in addition to the qualitative histopathological examination of pituitary sections. None of these investigations uncovered any difference between the two groups.

Aip mice were previously shown to exhibit full penetrance of pituitary tumors by the age of 15 months and an approximately 80% penetrance by the age of 12 months (4); hence, to enable a good discrimination of pituitary pathological findings between the two genotypes studied while avoiding a bias due to the coincidence of sporadic pituitary tumors frequently found in older mice, we chose to focus on the age group of 12 months in the present study. Other later research similarly did not detect any overt pituitary tumors in the same Aip heterozygous mouse model at 12 months of age (32).

The possible explanations for this include 1. a later manifestation of a pituitary tumor phenotype, 2. a lower penetrance of *Aip*-dependent pituitary tumors, or 3. a less severe pituitary phenotype (i.e. only subtle hypertrophy) in our Aip mice. In contrast to the previously described complete penetrance in murine *Aip*-dependent pituitary tumor formation (4), large clinical studies estimate the penetrance of pathogenic *AIP* variants in humans to be around 20% (3,41,42).

It is known that somatropinoma formation is often preceded by a long period of somatotroph hyperplasia in humans with Carney complex and that clinical and biochemical acromegaly in humans can occur in the absence of radiologically or even histologically detectable somatotroph adenomas (43–45). It is therefore possible, and considering the phenotypic changes and elevated IGF-1 levels, indeed likely, that pituitary GH secretion in our 12-month-old Aip mice was already increased as a sign of the very early stages of somatotropinoma formation, but subtle signs of somatotroph hyperplasia were not yet evident on histopathology. An elevated GH releasing hormone (GHRH) sensitivity of $Aip^{+/-}$ pituitaries in terms of GH release was already shown at the age of 3 months (32), confirming that this genotype causes subtle changes in somatotroph function for a long period of time; the clear phenotypic difference in our 12-month-old mice might reflect the cumulative effects of long-standing but small differences in somatotroph GH release. Moreover, somatotroph GH synthesis (transcription and translation) and GH release are two processes that are governed by different intracellular signaling pathways: GH transcription is stimulated by the PKA/CREB-dependent transcription-factor Pit1, whereas GH release from intracellular storage vesicles is regulated via PKA-dependent calcium influx as well as PKA-independent effects (46). A rapid release of GH from intracellular stores in connection with a slower upregulation of cellular synthesis could preclude the immunohistochemical detection of any elevation of intracellular GH levels by GH staining.

Other groups studying the same Aip-deficient mouse model found an increased total GH secretion and an increased pituitary *ex vivo* response to GHRH compared with wt mice, and similarly no pituitary adenomas were identified at 12 months of age (32). A notably slow progression from pituitary hyperplasia to adenoma formation was even observed in the pituitaries of somatotroph-specific *Aip* knockout mice (31). An increased release of GH in the absence of somatotropinomas in our Aip mice bears important implications for the medical treatment of human $AIPmut^{+}$ acromegaly and gigantism, suggesting that targeting the production or release of GH may allow an earlier or more efficacious treatment than an inhibition of somatotroph proliferation. Research suggests a differential response of somatostatin analog treatment in relation to somatotroph AIP expression in sporadic acromegaly (47).

To exclude any effect of different genetic backgrounds on the differences between the groups of mice observed in the current study, the Aip mice—originally generated in a C57BL/6Rcc background—were crossed with *Prkar1a* haploinsufficient mice available in our laboratory, which were maintained on a C57BL/6/129Sv hybrid background (48). Conversely, however, we cannot exclude that this mixed background contributed to differences in onset or severity of Aip-dependent pituitary adenomas in our Aip mice compared with the Aip mice examined in the original publication (4). In human sporadic acromegaly, cellular AIP levels were shown to be regulated by miRNAs (49,50), and the investigation of genetic susceptibility to FIPA has implicated a number of modifier loci (51), so it is possible that the difference in a genetic background led to a lower susceptibility to Aip-dependent tumorigenesis in our mice. Supporting this hypothesis, even in somatotroph-specific *Aip* knockout mice, somatotroph tumor formation was only detected at the age of 40 weeks, thus suggesting that other additional factors are required for tumor formation (31). Similarly, human *AIP*-dependent FIPA has a relatively low disease penetrance while patients with Carney complex present with a heterogeneous phenotype concerning type and time of disease manifestations. It is conceivable that modulations in AIP expression or function could influence the clinical presentation of Carney complex patients, whereas PKA pathway alterations including germline or somatic *PRKAR1A* variants could exert an effect on the penetrance of *AIP*-dependent FIPA. This aspect may be interesting to investigate in the tumors of affected patients.

Since both *Aip* and *Prkar1a* haploinsufficiency separately lead to an increase in pituitary tumor propensity in mice and human, we hypothesized that the combined effects would cause a higher frequency or severity of somatotropinomas and acromegalic features in our double heterozygous Aip/R1α mice. On the contrary though, we observed that these mice had lower biochemical and phenotypic signs of GH excess. While some characteristics of these Aip/R1α mice are clearly mainly caused by the *Prkar1a* deficiency [e.g. frequent tail tumors most likely leading to the significantly reduced tail lengths or increased alkaline phosphatase levels probably reflecting the high tumor load in

these mice (9)], a smaller body size or lower cholesterol and triglyceride values have not been observed in *Prkar1a*$^{+/-}$ mice in comparison to wt mice. Conversely, we also did not observe an aggravation of the tumor phenotype of the *Prkar1a*$^{+/-}$ mouse by a combination with Aip heterozygosity. We suggest that the growth plate thickening observed in our 12-month-old Aip mice is unrelated to the bone lesions in R1α mice, since those have been shown to originate from an area adjacent to the growth plate (52). In addition, direct and indirect actions of circulating GH and IGF-1 on bone growth and the epiphyseal plate are well documented (53,54).

We suggest that this unexpected observation of a less severe acromegalic phenotype in Aip/R1α mice can be mechanistically explained by an imbalance of Aip binding to R1α and/or the main PKA catalytic subunit Cα. In the inactive state of the PKA, two catalytic and two regulatory subunits are bound to each other. Upon activation of the PKA pathway, the holoenzyme dissociates into the active catalytic subunits and the regulatory subunits (Fig. 5A). We demonstrated a physical interaction of Aip with R1α and Cα both in complex and separately (15), whereas others have found an interaction of Aip with Cα but not R1α (16), suggesting that there may be different affinities or dynamics of Aip binding to Cα and R1α. Reduced Aip levels lead to PKA pathway activation in somatotrope cells (13,15) and to somatotropinoma formation and mild GH excess in mice (4,31,32). In this situation, the lower amount of intracellular Aip may have a higher binding affinity for R1α and/or the inactive holoenzyme rather than unbound Cα, thereby leaving it in a highly active state (Fig. 5B). Under reduced Aip and R1α levels, Aip normally bound to R1α may relocate to Cα and inhibit its function, or to the holoenzyme and impede its dissociation, thereby causing an overall lower PKA pathway activity (Fig. 5C). While we did not detect any difference between Aip and Aip/R1α mice in immunohistochemical cAMP staining or phospho-CREB immunofluorescence, we suggest that this lack of documented difference does not preclude a subtly altered PKA pathway activity over a potentially long period of time. It would be interesting to specifically investigate the physical and functional aspects of an interaction between the PKA pathway and Aip in this mouse model by biochemical techniques including co-immunoprecipitation or PKA activation; however, these techniques are limited by the small amount of protein present in mouse pituitary gland.

In conclusion, we show here that *Aip*$^{+/-}$ mice have a GH excess phenotype which mirrors that of human acromegaly, including significantly elevated IGF-1 levels, without histopathological pituitary abnormalities. This phenotype is ameliorated in double heterozygous *Aip*$^{+/-}$, *Prkar1a*$^{+/-}$ mice, potentially due to changes in the binding dynamics between Aip and R1α as well as Cα. These findings support the notion that multiple environmental and genetic factors contribute to the acromegalic phenotype as well as to somatotroph tumor development, and they highlight the complexity of physical and functional interaction between Aip and the PKA pathway, including the catalytic and regulatory PKA subunits.

Materials and Methods

Animals

Mice were housed with ad libitum access to food and water on 12 h light/dark cycle. *Prkar1a*$^{+/-}$ mice carrying a deletion of exon 2 were generated in our laboratory, as described previously (9). *Aip*$^{+/-}$ mice, containing a gene trap vector construct in the intronic region between *Aip* exons 2 and 3, were kindly provided by Prof. Karhu (University of Helsinki) and were described previously (4). Homozygous null mutations in *Aip* and *Prkar1a* in mice are both embryonic lethal (4,9,33); *Aip*$^{+/-}$ mice and *Prkar1a*$^{+/-}$ mice were crossed and maintained on a C57BL/6129Sv/B6 hybrid background. Double heterozygous (*Aip*$^{+/-}$, *Prkar1a*$^{+/-}$) offspring were compared with single heterozygous *Aip*$^{+/-}$ mice at ages 3, 6, 9 and 12 months. Body weights were recorded monthly for all animals.

Animal studies were performed under protocol ASP12-033 and were approved by the *Eunice Kennedy Shriver* National Institute of Child Health and Human Development Institutional Animal Care and Use Committee.

Genotyping

For all animals, genotyping was performed from tail DNA by PCR. For *Prkar1a*, three primers (5′-AGCTAGCTTGGCTGGACG TA-3′, 5′-AAGCAGGCGAGCTATTAGTTTAT-3′ and 5′-CATCCATCT-CCTATCCCCTTT-3′) were used, where the wt allele led to a 242 bp product and the null allele to a 180 bp fragment (Supplementary Material, Fig. S1A). *Aip* genotyping was performed as described (4); the wt allele led to a 177 bp fragment, whereas a 193 bp fragment was created from the mutant allele (Supplementary Material, Fig. S1B).

Histopathological evaluation

Male and female single heterozygous *Aip*$^{+/-}$ and double heterozygous *Aip*$^{+/-}$, *Prkar1a*$^{+/-}$ mice were sacrificed at the ages of 3 ($n=12$), 6 ($n=12$), 9 ($n=12$) and 12 months ($n=23$). Terminal blood was collected by cardiac puncture; clinical chemistry and hematology were immediately analyzed by standard protocols. Gross pathological analysis, organ weights (thymus, heart, spleen, liver, kidneys and brain) and body lengths were recorded immediately.

Organs and tissues were then formalin fixed and paraffin embedded, sectioned onto glass slides and histopathological analysis was performed on hematoxylin/eosin (H&E)-stained sections by standard procedures (Histoserv, Inc., Germantown, MD).

Immunohistochemistry and immunofluorescence

Pituitaries were further analyzed by immunohistochemistry and immunofluorescence. Briefly, sections were deparaffinized and rehydrated in an ethanol dilution series, followed by heat-induced antigen retrieval. The primary antibodies were rabbit anti-rat GH (1:400) (Dr AF Parlow, National Hormone and Peptide Program, Harbor-UCLA Medical Center, Torrance, CA, USA), rabbit anti-Ki67 (ab15580, Abcam, Cambridge, UK, 1:500), anti-phospho-CREB (ab32096, Abcam, 1:150) and anti-cAMP (07-1497, Millipore, Burlington, MA, 1:100). For GH and Ki67 staining, antigen retrieval was performed by the Envision Flex target retrieval solution (high pH) (Agilent, Santa Clara, CA, USA) at 95°C for 20 min, followed by antibody incubation for 60 min at room temperature and detection by the Flex+ (rabbit) detection kit (Agilent) on a Dako autostainer system according to manufacturer's recommendations.

For phospho-CREB and cAMP immunohistochemistry, antigen retrieval was performed using a *Tris*-based antigen unmasking solution (Vector laboratories, Burlingame, CA, USA) at 100°C for 20 min followed by primary antibody incubation at 4°C overnight. For Phospho-CREB immunofluorescence, an Alexa Fluor (555) donkey-anti rabbit secondary antibody (Invitrogen,

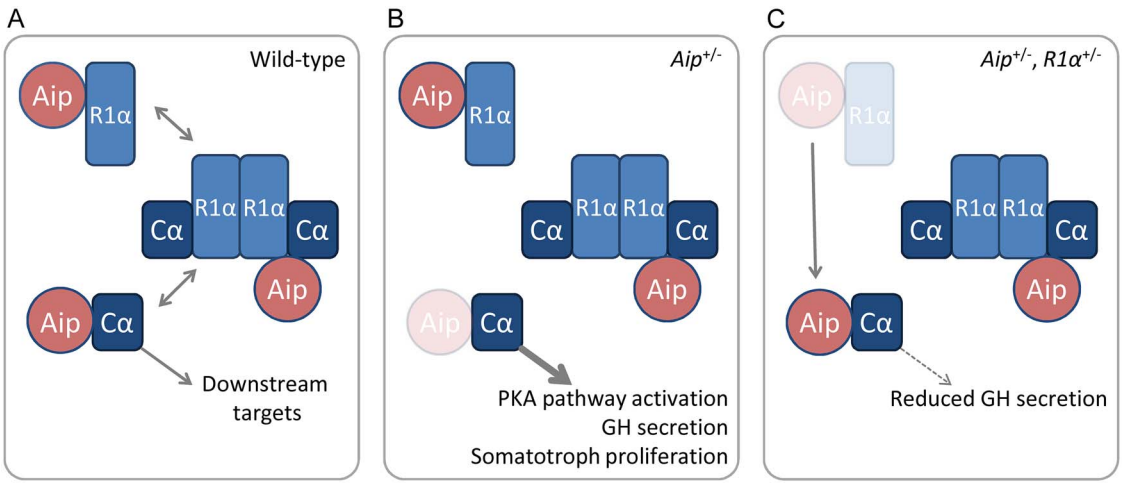

Figure 5. Schematic model of the binding dynamics of Aip with R1α and Cα in somatotrophs of different mouse models, contributing to GH secretion and somatotropinoma formation. (**A**) In the wild-type mouse, the inactive cAMP-dependent protein kinase (PKA) holoenzyme separates into its subunits upon PKA pathway activation, where the active catalytic subunit Cα exerts its downstream effects. Aip can bind the holoenzyme as well as the unbound catalytic and regulatory (R1α) subunits, probably with different affinities. (**B**) During lower Aip levels, e.g. in the *Aip*$^{+/-}$ mouse, Aip binding to unbound Cα may be reduced thereby freeing Cα for an increased activation of downstream targets, leading to more PKA pathway activation, increased GH secretion and somatotroph tumor formation. (**C**) In the double heterozygous *Aip*$^{+/-}$, *Prkar1a*$^{+/-}$ mouse, Aip that was previously bound to unbound R1α may now be free to bind to Cα, thereby inhibiting its catalytic activity and reducing GH secretion.

Carlsbad, CA, USA) was used and slides were mounted with DAPI Prolong Gold (Invitrogen). cAMP was detected by the ImmPRESS anti-rabbit detection kit (Vector laboratories).

Pituitary sections of all available 12-month-old mice were qualitatively and semi-quantitatively evaluated. Eosinophilia was scored using H&E stained slides on a scale from 0 (low) to 2 (high). Ki67 positivity was scored on a scale from 1 to 4 (<1, 1–2, 2–5, and 5–10%); both were performed by one blinded viewer (TR). Evaluation of GH expression was performed by two blinded viewers (MHSR and TR) who independently rated staining intensity on a scale from 1 to 5 (intermediate to very strong).

Insulin-like growth factor 1 measurements

Blood samples for IGF-1 analysis were obtained between 8 and 10 a.m. by tail venipuncture in male and female single and double heterozygous mice at the ages indicated. Serum was separated and stored at −20°C for later use. Samples were diluted 1:300 (for ages 18 and 28 weeks) or 1:50 (for age 49 weeks) and analyzed in duplicate by IGF-1 ELISA (Boster Biotech EK0378 for ages 18 and 28 weeks or ALPCO 22-IG1MS-E01 for age 49 weeks) according to manufacturer's instructions.

Statistics

Data were tested for normality using the Shapiro–Wilk test. Groups were compared using independent samples Student's *t*-tests, two-way ANOVA or Mann–Whitney-U tests, as appropriate. Differences in frequency were tested using two-sided Chi-squared tests. Data shown are means ± standard error of the mean or medians ± interquartile range or *n* as stated.

Supplementary Material

Supplementary Material is available at *HMG* online.

Acknowledgements

We thank Professor A. Karhu (University of Helsinki) for kindly providing the *Aip*$^{+/-}$ mice and I. Erber (Medical University of Vienna) for expert technical assistance with immunohistochemistry.

Conflict of Interest statement. Dr. Stratakis and Dr Trivellin report that they hold patents on technologies involving GPR101, and Dr. Stratakis holds patents on the function of the PRKAR1A and PDE11A genes. His laboratory has also received funding from Pfizer, Inc. on the treatment of gigantism and acromegaly, as well as a research project on growth hormone production, different than what is being reported here.

Funding

Intramural Research Program, NICHD, National Institutes of Health; Erwin Schrödinger Fellowship (grant number J3482-B13) by the Austrian Science Fund (FWF) to M.H.S.-R.

References

1. Melmed, S. (2003) Mechanisms for pituitary tumorigenesis: the plastic pituitary. *J. Clin. Invest.*, **112**, 1603–1618.
2. Vierimaa, O., Georgitsi, M., Lehtonen, R., Vahteristo, P., Kokko, A., Raitila, A., Tuppurainen, K., Ebeling, T.M., Salmela, P.I., Paschke, R. *et al.* (2006) Pituitary adenoma predisposition caused by germline mutations in the AIP gene. *Science*, **312**, 1228–1230.
3. Daly, A.F., Tichomirowa, M.A., Petrossians, P., Heliovaara, E., Jaffrain-Rea, M.L., Barlier, A., Naves, L.A., Ebeling, T., Karhu, A., Raappana, A. *et al.* (2010) Clinical characteristics and therapeutic responses in patients with germline AIP mutations and pituitary adenomas: an international collaborative study. *J. Clin. Endocrinol. Metab.*, **95**, E373–E383.

4. Raitila, A., Lehtonen, H.J., Arola, J., Heliovaara, E., Ahlsten, M., Georgitsi, M., Jalanko, A., Paetau, A., Aaltonen, L.A. and Karhu, A. (2010) Mice with inactivation of aryl hydrocarbon receptor-interacting protein (Aip) display complete penetrance of pituitary adenomas with aberrant ARNT expression. *Am. J. Pathol.*, **177**, 1969–1976.
5. Vallar, L., Spada, A. and Giannattasio, G. (1987) Altered Gs and adenylate cyclase activity in human GH-secreting pituitary adenomas. *Nature*, **330**, 566–568.
6. Landis, C.A., Harsh, G., Lyons, J., Davis, R.L., McCormick, F. and Bourne, H.R. (1990) Clinical characteristics of acromegalic patients whose pituitary tumors contain mutant Gs protein. *J. Clin. Endocrinol. Metab.*, **71**, 1416–1420.
7. Kirschner, L.S., Carney, J.A., Pack, S.D., Taymans, S.E., Giatzakis, C., Cho, Y.S., Cho-Chung, Y.S. and Stratakis, C.A. (2000) Mutations of the gene encoding the protein kinase a type I-alpha regulatory subunit in patients with the Carney complex. *Nat. Genet.*, **26**, 89–92.
8. Stratakis, C.A., Kirschner, L.S. and Carney, J.A. (2001) Clinical and molecular features of the Carney complex: diagnostic criteria and recommendations for patient evaluation. *J. Clin. Endocrinol. Metab.*, **86**, 4041–4046.
9. Kirschner, L.S., Kusewitt, D.F., Matyakhina, L., Towns, W.H., 2nd, Carney, J.A., Westphal, H. and Stratakis, C.A. (2005) A mouse model for the Carney complex tumor syndrome develops neoplasia in cyclic AMP-responsive tissues. *Cancer Res.*, **65**, 4506–4514.
10. Yin, Z., Williams-Simons, L., Parlow, A.F., Asa, S. and Kirschner, L.S. (2008) Pituitary-specific knockout of the Carney complex gene Prkar1a leads to pituitary tumorigenesis. *Mol. Endocrinol.*, **22**, 380–387.
11. Almeida, M.Q., Muchow, M., Boikos, S., Bauer, A.J., Griffin, K.J., Tsang, K.M., Cheadle, C., Watkins, T., Wen, F., Starost, M.F. *et al.* (2010) Mouse Prkar1a haploinsufficiency leads to an increase in tumors in the Trp53+/− or Rb1+/− backgrounds and chemically induced skin papillomas by dysregulation of the cell cycle and Wnt signaling. *Hum. Mol. Genet.*, **19**, 1387–1398.
12. Trivellin, G. and Korbonits, M. (2011) AIP and its interacting partners. *J. Endocrinol.*, **210**, 137–155.
13. Formosa, R., Xuereb-Anastasi, A. and Vassallo, J. (2013) Aip regulates cAMP signalling and GH secretion in GH3 cells. *Endocr. Relat. Cancer*, **20**, 495–505.
14. Tuominen, I., Heliovaara, E., Raitila, A., Rautiainen, M.R., Mehine, M., Katainen, R., Donner, I., Aittomaki, V., Lehtonen, H.J., Ahlsten, M. *et al.* (2015) AIP inactivation leads to pituitary tumorigenesis through defective Galphai-cAMP signaling. *Oncogene*, **34**, 1174–1184.
15. Schernthaner-Reiter, M.H., Trivellin, G. and Stratakis, C.A. (2018) Interaction of AIP with protein kinase a (cAMP-dependent protein kinase). *Hum. Mol. Genet.*, **27**, 2604–2613.
16. Hernandez-Ramirez, L.C., Morgan, R.M.L., Barry, S., D'Acquisto, F., Prodromou, C. and Korbonits, M. (2018) Multi-chaperone function modulation and association with cytoskeletal proteins are key features of the function of AIP in the pituitary gland. *Oncotarget*, **9**, 9177–9198.
17. Bolger, G.B., Bizzi, M.F., Pinheiro, S.V., Trivellin, G., Smoot, L., Accavitti, M.A., Korbonits, M. and Ribeiro-Oliveira, A., Jr. (2016) cAMP-specific PDE4 phosphodiesterases and AIP in the pathogenesis of pituitary tumors. *Endocr. Relat. Cancer*, **23**, 419–431.
18. Nakata, A., Urano, D., Fujii-Kuriyama, Y., Mizuno, N., Tago, K. and Itoh, H. (2009) G-protein signalling negatively regulates the stability of aryl hydrocarbon receptor. *EMBO Rep.*, **10**, 622–628.
19. Vilar, L., Vilar, C.F., Lyra, R., Lyra, R. and Naves, L.A. (2017) Acromegaly: clinical features at diagnosis. *Pituitary*, **20**, 22–32.
20. Nilsson, O., Marino, R., De Luca, F., Phillip, M. and Baron, J. (2005) Endocrine regulation of the growth plate. *Horm. Res.*, **64**, 157–165.
21. Palmer, A.J., Chung, M.Y., List, E.O., Walker, J., Okada, S., Kopchick, J.J. and Berryman, D.E. (2009) Age-related changes in body composition of bovine growth hormone transgenic mice. *Endocrinology*, **150**, 1353–1360.
22. Lenders, N.F., McCormack, A.I. and Ho, K.K.Y. (2020) Management of endocrine disease: does gender matter in the management of acromegaly? *Eur. J. Endocrinol.*, **182**, R67–R82.
23. Thorngren, K.G. and Hansson, L.I. (1973) Cell kinetics and morphology of the growth plate in the normal and hypophysectomized rat. *Calcif. Tissue Res.*, **13**, 113–129.
24. Colao, A., Marzullo, P., Vallone, G., Marino, V., Annecchino, M., Ferone, D., De Brasi, D., Scarpa, R., Oriente, P. and Lombardi, G. (1998) Reversibility of joint thickening in acromegalic patients: an ultrasonography study. *J. Clin. Endocrinol. Metab.*, **83**, 2121–2125.
25. Kopchick, J.J., Bellush, L.L. and Coschigano, K.T. (1999) Transgenic models of growth hormone action. *Annu. Rev. Nutr.*, **19**, 437–461.
26. Frick, F., Bohlooly, Y.M., Linden, D., Olsson, B., Tornell, J., Eden, S. and Oscarsson, J. (2001) Long-term growth hormone excess induces marked alterations in lipoprotein metabolism in mice. *Am. J. Physiol. Endocrinol. Metab.*, **281**, E1230–E1239.
27. Olsson, B., Bohlooly, Y.M., Fitzgerald, S.M., Frick, F., Ljungberg, A., Ahren, B., Tornell, J., Bergstrom, G. and Oscarsson, J. (2005) Bovine growth hormone transgenic mice are resistant to diet-induced obesity but develop hyperphagia, dyslipidemia, and diabetes on a high-fat diet. *Endocrinology*, **146**, 920–930.
28. Pivonello, R., Auriemma, R.S., Grasso, L.F., Pivonello, C., Simeoli, C., Patalano, R., Galdiero, M. and Colao, A. (2017) Complications of acromegaly: cardiovascular, respiratory and metabolic comorbidities. *Pituitary*, **20**, 46–62.
29. Guo, J., Jou, W., Gavrilova, O. and Hall, K.D. (2009) Persistent diet-induced obesity in male C57BL/6 mice resulting from temporary obesigenic diets. *PLoS One*, **4**, e5370.
30. Otto, G.P., Rathkolb, B., Oestereicher, M.A., Lengger, C.J., Moerth, C., Micklich, K., Fuchs, H., Gailus-Durner, V., Wolf, E. and Hrabe de Angelis, M. (2016) Clinical chemistry reference intervals for C57BL/6J, C57BL/6N, and C3HeB/FeJ mice (Mus musculus). *J. Am. Assoc. Lab. Anim. Sci.*, **55**, 375–386.
31. Gillam, M.P., Ku, C.R., Lee, Y.J., Kim, J., Kim, S.H., Lee, S.J., Hwang, B., Koo, J., Kineman, R.D., Kiyokawa, H. *et al.* (2017) Somatotroph-specific Aip-deficient mice display Pretumorigenic alterations in cell-cycle signaling. *J. Endocr. Soc*, **1**, 78–95.
32. Lecoq, A.L., Zizzari, P., Hage, M., Decourtye, L., Adam, C., Viengchareun, S., Veldhuis, J.D., Geoffroy, V., Lombes, M., Tolle, V. *et al.* (2016) Mild pituitary phenotype in 3- and 12-month-old Aip-deficient male mice. *J. Endocrinol.*, **231**, 59–69.
33. Lin, B.C., Sullivan, R., Lee, Y., Moran, S., Glover, E. and Bradfield, C.A. (2007) Deletion of the aryl hydrocarbon receptor-associated protein 9 leads to cardiac malformation and embryonic lethality. *J. Biol. Chem.*, **282**, 35924–35932.

34. Kelley, K.W., Brief, S., Westly, H.J., Novakofski, J., Bechtel, P.J., Simon, J. and Walker, E.B. (1986) GH3 pituitary adenoma cells can reverse thymic aging in rats. *Proc. Natl. Acad. Sci. U. S. A.*, **83**, 5663–5667.
35. French, R.A., Broussard, S.R., Meier, W.A., Minshall, C., Arkins, S., Zachary, J.F., Dantzer, R. and Kelley, K.W. (2002) Age-associated loss of bone marrow hematopoietic cells is reversed by GH and accompanies thymic reconstitution. *Endocrinology*, **143**, 690–699.
36. Souadjian, J.V., Molnar, G.D., Silverstein, M.N. and Titus, J.L. (1970) Morphologic studies of the thymus in acromegaly, diabetes mellitus, and Cushing's syndrome. *Metabolism*, **19**, 401–405.
37. Golde, D.W., Bersch, N. and Li, C.H. (1977) Growth hormone: species-specific stimulation of erythropoiesis in vitro. *Science*, **196**, 1112–1113.
38. Kurtz, A., Zapf, J., Eckardt, K.U., Clemons, G., Froesch, E.R. and Bauer, C. (1988) Insulin-like growth factor I stimulates erythropoiesis in hypophysectomized rats. *Proc. Natl. Acad. Sci. U. S. A.*, **85**, 7825–7829.
39. Christ, E.R., Cummings, M.H., Westwood, N.B., Sawyer, B.M., Pearson, T.C., Sonksen, P.H. and Russell-Jones, D.L. (1997) The importance of growth hormone in the regulation of erythropoiesis, red cell mass, and plasma volume in adults with growth hormone deficiency. *J. Clin. Endocrinol. Metab.*, **82**, 2985–2990.
40. Strauch, G., Lego, A., Therain, F. and Bricaire, H. (1977) Reversible plasma and red blood cells volumes increases in acromegaly. *Acta Endocrinol.*, **85**, 465–478.
41. Hernandez-Ramirez, L.C., Gabrovska, P., Denes, J., Stals, K., Trivellin, G., Tilley, D., Ferrau, F., Evanson, J., Ellard, S., Grossman, A.B. *et al.* (2015) Landscape of familial isolated and young-onset pituitary adenomas: prospective diagnosis in AIP mutation carriers. *J. Clin. Endocrinol. Metab.*, **100**, E1242–E1254.
42. Igreja, S., Chahal, H.S., King, P., Bolger, G.B., Srirangalingam, U., Guasti, L., Chapple, J.P., Trivellin, G., Gueorguiev, M., Guegan, K. *et al.* (2010) Characterization of aryl hydrocarbon receptor interacting protein (AIP) mutations in familial isolated pituitary adenoma families. *Hum. Mut.*, **31**, 950–960.
43. Pack, S.D., Kirschner, L.S., Pak, E., Zhuang, Z., Carney, J.A. and Stratakis, C.A. (2000) Genetic and histologic studies of somatomammotropic pituitary tumors in patients with the "complex of spotty skin pigmentation, myxomas, endocrine overactivity and schwannomas" (Carney complex). *J. Clin. Endocrinol. Metab.*, **85**, 3860–3865.
44. Raff, S.B., Carney, J.A., Krugman, D., Doppman, J.L. and Stratakis, C.A. (2000) Prolactin secretion abnormalities in patients with the "syndrome of spotty skin pigmentation, myxomas, endocrine overactivity and schwannomas" (Carney complex). *J. Pediatr. Endocrinol. Metab.*, **13**, 373–379.
45. Garcia, M.B., Koppeschaar, H.P., Lips, C.J., Thijssen, J.H. and Krenning, E.P. (1994) Acromegaly and hyperprolactinemia in a patient with polyostotic fibrous dysplasia: dynamic endocrine studies and treatment with the somatostatin analogue octreotide. *J. Endocrinol. Investig.*, **17**, 59–65.
46. Schernthaner-Reiter, M.H., Trivellin, G. and Stratakis, C.A. (2020) Chaperones, somatotroph tumors and the cyclic AMP (cAMP)-dependent protein kinase (PKA) pathway. *Mol. Cell. Endocrinol.*, **499**, 110607.
47. Kasuki, L., Vieira Neto, L., Wildemberg, L.E., Colli, L.M., de Castro, M., Takiya, C.M. and Gadelha, M.R. (2012) AIP expression in sporadic somatotropinomas is a predictor of the response to octreotide LAR therapy independent of SSTR2 expression. *Endocr. Relat. Cancer*, **19**, L25–L29.
48. Saloustros, E., Salpea, P., Qi, C.F., Gugliotti, L.A., Tsang, K., Liu, S., Starost, M.F., Morse, H.C., 3rd and Stratakis, C.A. (2015) Hematopoietic neoplasms in Prkar2a-deficient mice. *J. Exp. Clin. Cancer Res.*, **34**, 143.
49. Denes, J., Kasuki, L., Trivellin, G., Colli, L.M., Takiya, C.M., Stiles, C.E., Barry, S., de Castro, M., Gadelha, M.R. and Korbonits, M. (2015) Regulation of aryl hydrocarbon receptor interacting protein (AIP) protein expression by MiR-34a in sporadic somatotropinomas. *PLoS One*, **10**, e0117107.
50. Trivellin, G., Butz, H., Delhove, J., Igreja, S., Chahal, H.S., Zivkovic, V., McKay, T., Patocs, A., Grossman, A.B. and Korbonits, M. (2012) MicroRNA miR-107 is overexpressed in pituitary adenomas and inhibits the expression of aryl hydrocarbon receptor-interacting protein in vitro. *Am. J. Physiol. Endocrinol. Metab.*, **303**, E708–E719.
51. Toledo, R.A., Lourenco, D.M., Jr. and Toledo, S.P.A. (2010) Familial isolated pituitary adenoma: evidence for genetic heterogeneity. *Front. Horm. Res.*, **38**, 77–86.
52. Tsang, K.M., Starost, M.F., Nesterova, M., Boikos, S.A., Watkins, T., Almeida, M.Q., Harran, M., Li, A., Collins, M.T., Cheadle, C. *et al.* (2010) Alternate protein kinase a activity identifies a unique population of stromal cells in adult bone. *Proc. Natl. Acad. Sci. U. S. A.*, **107**, 8683–8688.
53. Isaksson, O.G., Jansson, J.O. and Gause, I.A. (1982) Growth hormone stimulates longitudinal bone growth directly. *Science*, **216**, 1237–1239.
54. Lupu, F., Terwilliger, J.D., Lee, K., Segre, G.V. and Efstratiadis, A. (2001) Roles of growth hormone and insulin-like growth factor 1 in mouse postnatal growth. *Dev. Biol.*, **229**, 141–162.